Letter

Critical scaling of compression-driven jamming of athermal frictionless spheres in suspension

Anton Peshkov and S. Teitel
Department of Physics and Astronomy, University of Rochester, Rochester, New York 14627, USA

(Received 19 October 2020; revised 7 January 2021; accepted 8 March 2021; published 2 April 2021)

We study numerically a system of athermal, overdamped, frictionless spheres, as in a non-Brownian suspension, in two and three dimensions. Compressing the system isotropically at a fixed rate $\dot{\epsilon}$, we investigate the critical behavior at the jamming transition. The finite compression rate introduces a control timescale, which allows one to probe the critical timescale associated with jamming. As was found previously for steady-state shear-driven jamming, we find for compression-driven jamming that pressure obeys a critical scaling relation as a function of packing fraction ϕ and compression rate $\dot{\epsilon}$, and that the bulk viscosity $p/\dot{\epsilon}$ diverges upon jamming. A scaling analysis determines the critical exponents associated with the compression-driven jamming transition. Our results suggest that stress-isotropic, compression-driven jamming may be in the same universality class as stress-anisotropic, shear-driven jamming.

DOI: 10.1103/PhysRevE.103.L040901

Athermal granular and related soft matter materials, such as non-Brownian suspensions, emulsions, and foams, all undergo a phase transition from a liquidlike state to a rigid disordered state as the packing fraction ϕ of the granular particles increases. This is the jamming transition [1,2]. Here we focus on the behavior of frictionless particles, where jamming is like a continuous phase transition with respect to the behavior of the stress. Early studies of jamming focused on what we will call stress-isotropic jamming: mechanically stable jammed configurations are generated by isotropically compressing the system, or by energy quenching random initial configurations at fixed ϕ [2–6]. At low ϕ, particles avoid each other and the pressure p vanishes. At a critical ϕ_J, a system-spanning rigid cluster forms and the pressure becomes finite, while the shear stress σ remains zero. Later studies investigated shear-driven jamming [7–16], where the system is uniformly sheared at a fixed strain rate $\dot{\gamma}$. For systems with a Newtonian rheology, such as particles in suspension, the system flows at low ϕ and small $\dot{\gamma}$ with a shear stress $\sigma \propto \dot{\gamma}$. Thus, for $\dot{\gamma} \to 0$, the viscosity $\eta = \sigma/\dot{\gamma}$ remains finite. However, above a critical ϕ_J, the system develops a nonzero yield stress $\sigma_0(\phi) = \lim_{\dot{\gamma}\to 0} \sigma > 0$ leading to a diverging viscosity. Because of this finite σ, we will refer to this as stress-anisotropic jamming. Given the different symmetry of anisotropic shear-driven jamming versus isotropic compression-driven jamming, it is natural to wonder if they belong to the same critical universality class, i.e., if the critical exponents describing singular behaviors are the same for any given dimensionality of the system. For equilibrium critical points, different symmetries often imply different universality classes [17].

In this work, we consider this question by investigating the dynamical behavior of the unjammed state below ϕ_J in order to probe the diverging timescale associated with jamming. In particular, we numerically compute the bulk viscosity $\zeta = p/\dot{\epsilon}$ of frictionless, overdamped, soft-core particles, isotropically compressed at finite compression rates $\dot{\epsilon}$. Although isotropic compression causes the packing ϕ to steadily increase, and thus it does not produce a steady-state ensemble as does simple shearing, we nevertheless can compute ζ by averaging results over several different independent compression runs. Below jamming we find that ζ has a well-defined limit as $\dot{\epsilon} \to 0$, which diverges as $\phi \to \phi_J$. We demonstrate that a simple critical scaling ansatz, found previously to apply for shear-driven jamming [8,9], also applies to compression-driven jamming, thus uniting these two different thrusts of jamming research and providing a framework in which to numerically address the question of a common universality class. Our scaling analysis strongly suggests that the critical exponents of compression-driven jamming in two dimensions (2D) are the same as previously found for shear-driven jamming; the situation in three dimensions (3D) remains less clear.

Prior Works. Numerical works in 3D [18,19] have argued for a common universality for athermal isotropic and anisotropic jamming by looking at static "shear-jammed" configurations of soft-core spheres, obtained by applying a static shear strain to unjammed isotropic configurations, and increasing the shear strain until jamming occurs. The same scalings of pressure and contact number were obtained as were previously found in isotropic jamming [2]. Similar conclusions for *thermalized* hard-core spheres have been found in infinite-dimensional mean-field calculations [20] and in 3D simulations [19]. These works are concerned with the structural properties of static, mechanically stable configurations at or above jamming, and they do not probe the dynamics associated with a diverging timescale as one approaches jamming from below.

However, a connection between structural and dynamic properties was proposed in [21,22] using a marginal-stability analysis. If $\eta_p = p/\dot{\gamma}$ is the pressure analog of shear viscosity in a shear-driven steady state, then [21,22] argued that

the exponent β, which characterizes the divergence of η_p as jamming is approached from below, is determined by the exponent θ that describes the distribution of small contact forces between particles in configurations exactly at jamming. In other works [23,24], this viscosity η_p was found to scale proportional to the decay time τ for a sheared configuration to relax to zero energy after the driving strain is turned off. Recently, a direct calculation [25] of τ from the dynamical matrix of jammed configurations was found to give the same relationship between τ and θ as in [21,22].

If these marginal-stability arguments are correct (see [26] for further discussion), and if the exponent θ has the same value in stress-isotropic jammed configurations as in stress-anisotropic jammed configurations, it could imply a common universality for dynamic behavior. Such a common value for θ was found for thermalized hard spheres at jamming in [19,20]. However, it remains unclear whether the properties of the thermally equilibrated, mechanically stable, shear-jammed states of [19,20] are necessarily the same as in the athermal, nonequilibrium, steady state of shear-driven jamming.

Experimental support for the critical scaling of shear-driven flow curves in 3D has been found in both non-Brownian suspensions [27,28] and emulsions [29–31]. However, the critical exponents $\beta \approx 1.7$-2 found in these works are significantly smaller than that given by the above theoretical prediction, $\beta = 2.83$ [26], possibly because the data used in these experiments span too wide a range of packing ϕ. We are unaware of any similar experimental investigations for the divergence of relaxation times or bulk viscosity in *athermal* compression-driven systems.

Recently, numerical simulations have been used to investigate dynamic behavior below the jamming ϕ_J. As a direct probe of diverging timescales upon approaching jamming from below, Ikeda *et al.* [32] measured the decay time τ as 3D configurations relax to zero energy according to overdamped equations of motion. For both stress-isotropic random initial configurations, and for stress-anisotropic initial configurations sampled from steady-state shearing, they found τ to collapse to a common curve, with a common divergence as $\phi \to \phi_J$, thus suggesting the same critical universality. However, a more recent work [33] by several of the same authors of [32] questions these results. While the predictions of [21,22,25], relating the divergence of τ to the force exponent θ, appear to hold for small system sizes, once the number of particles N in the system is sufficiently large, they found that $\tau \sim \ln N$ for $\phi < \phi_J$; thus τ would seem to have no proper thermodynamic limit. It is therefore important to reexamine this question numerically, using a method alternative to τ, to probe the timescale associated with jamming as $\phi \to \phi_J$ from below.

To do so, we consider here isotropic compression at a finite rate $\dot{\epsilon}$ [34] of soft-core, overdamped athermal spheres, as in a non-Brownian suspension, in both 2D and 3D. The finite rate $\dot{\epsilon}$ introduces a control time by which one can probe the timescale associated with jamming. Measuring the bulk viscosity $\zeta = p/\dot{\epsilon}$, we find no finite-size effect, as was claimed for τ in [33]. Considering soft spheres allows us to measure not only how ζ diverges below ϕ_J, but also how p behaves above ϕ_J. We can then compare these results against previous simulations of the viscosity η_p in the shear-driven steady-state.

Model. Our model consists of bidisperse, frictionless soft-core spheres, with equal numbers of big and small spheres with diameter ratio $d_b/d_s = 1.4$ [2]. For particles with center-of-mass positions $\mathbf{r}_i$, and $r_{ij} = |\mathbf{r}_i - \mathbf{r}_j|$, two particles interact with a one-sided harmonic contact potential, $U(r_{ij}) = \frac{1}{2}k_e(1 - r_{ij}/d_{ij})^2$, whenever their separation $r_{ij} < d_{ij} = (d_i + d_j)/2$. The elastic force on i, due to contact with j, is thus $\mathbf{f}_{ij}^{\rm el} = -dU(r_{ij})/d\mathbf{r}_i$, and the total elastic force on i is $\mathbf{f}_i^{\rm el} = \sum_j \mathbf{f}_{ij}^{\rm el}$, where the sum is over all j in contact with i. Particles also experience a dissipative drag force $\mathbf{f}_i^{\rm dis}$ with respect to a suspending host medium. We take $\mathbf{f}_i^{\rm dis} = -k_d V_i[\mathbf{v}_i - \mathbf{v}_{\rm host}(\mathbf{r}_i)]$, where V_i is the volume of particle i, and $\mathbf{v}_i = d\mathbf{r}_i/dt$. For uniform compression we define the local velocity of the host medium as $\mathbf{v}_{\rm host}(\mathbf{r}) = -\dot{\epsilon}\mathbf{r}$. This simple model has been widely used for sheared suspensions [7,8,10,15,21,22,35–40]. Particles obey the equation of motion, $m_i[d\mathbf{v}_i/dt] = \mathbf{f}_i^{\rm el} + \mathbf{f}_i^{\rm dis}$, where m_i is the mass of particle i, which we take proportional to its volume V_i.

To simulate our model, we use dimensionless units of length, energy, and time so that $d_s = 1$, $k_e = 1$, and $t_0 = (D/2)k_d V_s d_s^2/k_e = 1$, where $D = 2, 3$ is the dimensionality of the system. We define the quality factor $Q \equiv \tau_d/\tau_e = \sqrt{m_s k_e}/k_d V_s d_s$ as the ratio of the dissipative time $\tau_d = m_s/(k_d V_s)$ and the elastic time $\tau_e = \sqrt{m_s d_s^2/k_e}$ [41]. Note, $t_0 = (D/2)\tau_e/Q$. We set the mass of the small particles m_s so that $Q = 0.01$ in 2D and 0.0225 in 3D, which puts our system in the strongly overdamped limit $Q < 1$ where p is independent of Q [41]. We use LAMMPS [42] to integrate the equations of motion, using a time step of $\Delta t/t_0 = 0.01$. Our system consists of N particles in a cubic (square) box of length L. We compress by decreasing the box length at a fixed strain rate, $dL/dt = -\dot{\epsilon}L$, while the particles are acted on by the compressing host medium via $\mathbf{f}_i^{\rm dis}$. This results in an increasing packing fraction $\phi = N(V_s + V_b)/(2L^D)$. We take periodic boundary conditions in all directions. Compressing our system at rates from $\dot{\epsilon} = 10^{-5}$ down to $10^{-8.5}$, we measure the pressure p of the elastic forces from the stress tensor $L^{-D}\sum_{i<j} \mathbf{f}_{ij}^{\rm el} \otimes (\mathbf{r}_i - \mathbf{r}_j)$ as a function of the packing ϕ. To check for finite-size effects, we compare systems with $N =$ 16 384 and 32 768 particles, averaging over 10 independent random initial configurations for each size. Further details of our compression protocol can be found in our Supplemental Material [26].

Results. In Fig. 1 we plot our results for pressure p and bulk viscosity $\zeta = p/\dot{\epsilon}$ in both 2D and 3D. No finite-size effect is observed in our data (see Supplemental Material [26] for details). Our results are qualitatively similar to results seen for pressure and shear viscosity in shear-driven jamming [8,9]. From the trends observed as $\dot{\epsilon}$ decreases, our results suggest the following limiting behavior as $\dot{\epsilon} \to 0$: below ϕ_J, p vanishes while ζ approaches a constant; above ϕ_J, p stays finite while ζ diverges. As $\phi \to \phi_J$ from above, p vanishes continuously; as $\phi \to \phi_J$ from below, ζ diverges continuously, demonstrating the existence of a diverging timescale in compression-driven jamming. This is our first key result.

To confirm the above behavior, we posit that pressure obeys a critical scaling equation of the same form found in shear-driven jamming [7–10,38],

$$p = \dot{\epsilon}^q f(\delta\phi/\dot{\epsilon}^{1/z\nu}), \qquad \delta\phi \equiv \phi - \phi_J, \tag{1}$$

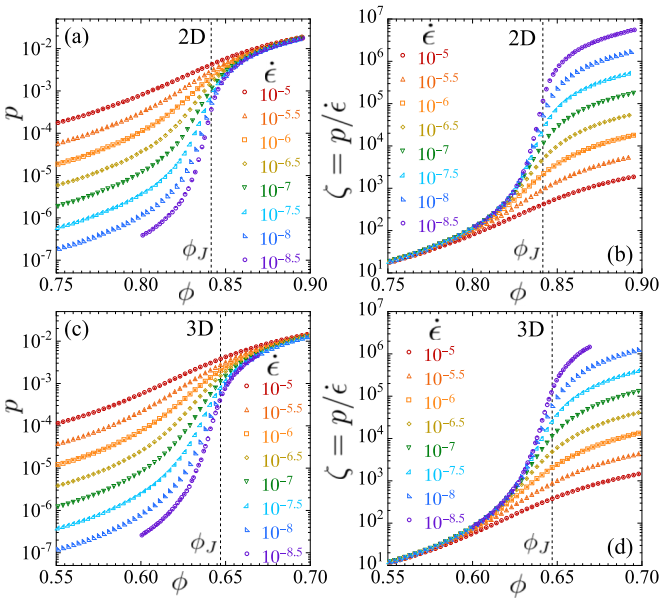

FIG. 1. (a) Pressure p and (b) bulk viscosity $\zeta = p/\dot\epsilon$ vs packing ϕ, for different compression rates $\dot\epsilon$ in two dimensions, and (c) p and (d) ζ in three dimensions. The vertical dashed lines locate the jamming ϕ_J. Results for $N = 16\,384$ particles are shown as open symbols, while results for $N = 32\,768$ are solid symbols. No dependence on N is observed. Error bars are roughly the size of the data symbols.

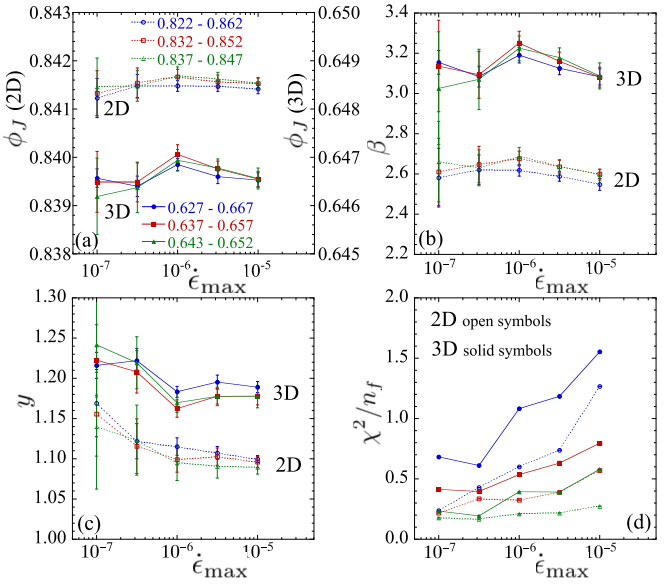

FIG. 2. Critical scaling parameters (a) ϕ_J, (b) β, (c) y, and (d) the χ^2/n_f of the fits, vs the upper limit of compression rate $\dot\epsilon_{\max}$ used in the fit, for three different ranges of $\phi \in [\phi_{\min}, \phi_{\max}]$. Each panel shows results for both 2D and 3D systems. We use the jackknife method to compute the estimated errors and bias-corrected averages of the fit parameters. The data symbols in all panels follow the legend shown in (a); open symbols and dotted lines are for 2D, solid symbols and solid lines are for 3D. Note in (a) that the scale for ϕ_J in 2D is on the left, while the scale for ϕ_J in 3D is on the right.

where $f(x)$ is an unknown scaling function. Since we observe that $\zeta = p/\dot\epsilon$ approaches a finite limit as $\dot\epsilon \to 0$ below ϕ_J, Eq. (1) implies that $f(x \to -\infty) \sim |x|^{-(1-q)z\nu}$, so that for $\phi < \phi_J$,

$$\lim_{\dot\epsilon \to 0} \zeta \sim |\phi - \phi_J|^{-\beta}, \qquad \beta = (1-q)z\nu. \tag{2}$$

Above ϕ_J, we observe that p approaches a finite limit as $\dot\epsilon \to 0$, so Eq. (1) implies that $f(x \to +\infty) \sim x^{qz\nu}$, so that for $\phi < \phi_J$,

$$\lim_{\dot\epsilon \to 0} p \sim (\phi - \phi_J)^{y}, \qquad y = qz\nu. \tag{3}$$

Note, the exponent β is expected to be independent of the specific form of the elastic contact potential since it describes behavior in the $\dot\epsilon \to 0$ hard-core limit [10]; the exponent y, however, is sensitive to the power-law of the contact potential [2,10]. A review of scaling in the context of shear-driven jamming may be found in [9].

Since we find no size dependence in our data, we average the results from our $N = 16\,384$ and $32\,768$ systems together, so as to improve our statistics. Expanding the log of the scaling function as a fifth-order polynomial, $\ln f(x) = \sum_{n=0}^{5} c_n x^n$, we fit our data to Eq. (1), regarding ϕ_J, q, $1/z\nu$, and the c_n as free fitting parameters.

The scaling form (1) holds only asymptotically close to the critical point, i.e., $\phi \to \phi_J$, $\dot\epsilon \to 0$. To test that our fits are stable and self-consistent, we fit to Eq. (1) using different windows of data, with $\phi \in [\phi_{\min}, \phi_{\max}]$ and $\dot\epsilon \leqslant \dot\epsilon_{\max}$, to see how our fitted parameters vary as we shrink the data window closer to the critical point. Since our polynomial expansion for the scaling function $f(x)$ should be good only for small x, we also restrict the data used in the fit to satisfy $|x| \leqslant 1$.

In Fig. 2 we show the results from such fits, comparing 2D and 3D systems. In Fig. 2(a) we show the jamming ϕ_J, in Fig. 2(b) the exponent β, in Fig. 2(c) the exponent y, and in Fig. 2(d) the χ^2/n_f of the fit, where n_f is the number of degrees of freedom of the fit. All quantities are plotted versus $\dot\epsilon_{\max}$ for three different ranges of $[\phi_{\min}, \phi_{\max}]$. We use the jackknife method to estimate errors (one standard deviation statistical error) and bias-corrected averages of these parameters. We see that the fitted parameters remain constant, within the estimated errors, as $\dot\epsilon_{\max}$ decreases and we vary the range of ϕ. This suggests that our fits are stable and self-consistent, with no need to include corrections-to-scaling in the analysis, such as has been found to be necessary for simple shearing [8,9]. The χ^2/n_f decrease as we narrow the window closer to the critical point; for our narrowest window in ϕ the χ^2/n_f remain roughly constant at the two smallest $\dot\epsilon_{\max}$, another indication of the good quality of our fits. It is difficult, however, to assess the significance of the numerical value of χ^2/n_f; unlike for shearing, where each data point $(\phi, \dot\gamma)$ represents an average over a steady-state shearing ensemble that is independent of its starting configuration [6], for compression the configuration at a given $(\phi, \dot\epsilon)$ is in general strongly correlated with the configuration at the previous compression step $(\phi - \Delta\phi, \dot\epsilon)$, and so the estimated errors on the data points are similarly correlated.

Figure 2 shows that the exponents β and y are different comparing 2D with 3D, in agreement with recent results for simple shearing [23]. Thus jamming criticality in 2D seems

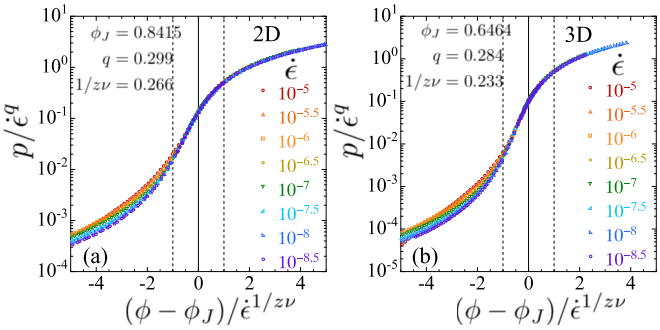

FIG. 3. Scaling collapses showing $p/\dot{\epsilon}$ vs $(\phi - \phi_J)/\dot{\epsilon}^{1/z\nu}$ for (a) our 2D system and (b) our 3D system. The values of ϕ_J, q, and $1/z\nu$ used in making these plots come from our fits for $\dot{\epsilon}_{\max} = 10^{-6.5}$ and the narrowest range of $[\phi_{\min}, \phi_{\max}]$. The points within this data window, which are used to make the fit, are shown as solid symbols; the points that are not used in the fit are shown as open symbols. We see a good collapse even for data that lie well outside the data window used in the fit. The vertical solid line locates the jamming $\delta\phi = 0$; the vertical dashed lines denote the additional constraint $|x| \leqslant 1$ for data used in the fit.

to be different from that in 3D. This is our second key result. Taking the fit for the narrowest range $[\phi_{\min}, \phi_{\max}]$ and $\dot{\epsilon}_{\max} = 10^{-6.5}$ as representative, we use those parameters to make a scaling collapse of our data in Fig. 3, plotting $p/\dot{\epsilon}^q$ versus $(\phi - \phi_J)/\dot{\epsilon}^{1/z\nu}$. We see an excellent data collapse, which extends well outside the data window that was use to determine the fit parameters. However, when $\delta\phi/\dot{\epsilon}^{1/z\nu} \lesssim -2$, we see that the data depart from a common scaling curve at the larger values of $\dot{\epsilon}$. We believe this is due to the effect of corrections-to-scaling that become more significant as $\dot{\epsilon}$ increases and one goes further from the critical point.

From the fits of Fig. 3 we find the following critical parameters. In 2D we have $\phi_J = 0.8415 \pm 0.0003$, $\beta = 2.63 \pm 0.09$, and $y = 1.12 \pm 0.04$. We can compare these to the values found in simple shearing, in which case β is the exponent associated with the divergence of the pressure analog of the shear viscosity, $\eta_p = p/\dot{\gamma}$. For shearing of the same model system as considered here, Ref. [8] gives $\phi_J = 0.8435 \pm 0.0002$, $\beta = 2.77 \pm 0.20$, and $y = 1.08 \pm 0.03$, while Ref. [10] gives $\phi_J = 0.8433 \pm 0.0001$, $\beta = 2.58 \pm 0.10$, and $y = 1.09 \pm 0.01$. We thus find that the values of the exponents β and y, found here for compression-driven jamming, agree completely, within the estimated errors, with those found for simple shearing. In 2D, compression-driven and shear-driven jamming appear to be in the same universality class. This is our third key result.

Note, our ϕ_J for compression-driven jamming is slightly lower than that found for shear-driven jamming. It is well known [4–6] that the value of ϕ_J can depend on the jamming protocol, and that the isotropic jamming ϕ_J found from rapid quenches of random initial configurations is lower than that found from shear-driven jamming. We can compare our ϕ_J for compression-driven jamming with previous values for isotropic rapid quenches. In [43], O'Hern *et al.* find $\phi_J = 0.842$, while in [44], Våberg *et al.* find $0.841\,77 \pm 0.000\,01$. Both agree, within the estimated errors, with our compression-driven value above.

For our 3D system, we find $\phi_J = 0.6464 \pm 0.0005$, $\beta = 3.07 \pm 0.15$, and $y = 1.22 \pm 0.03$. Our value of ϕ_J is a bit lower than the $\phi_J = 0.648$ found for the same model with the rapid quench protocol [43], and the $\phi_J = 0.6481$ found by Chaudhuri *et al.* [4] for a more complicated isotropic compression/decompression protocol that starts at a low ϕ_{init}; neither of these works give an estimate for the error in their values. As in 2D, our 3D compression-driven value of ϕ_J is slightly lower than values found for simple shearing of the same model, $\phi_J = 0.6474$ in [39] and [40], and $\phi_J = 0.6491 \pm 0.0001$ in [23].

Concerning the critical exponents in 3D models of overdamped sheared suspensions, numerical simulations on hard-core spheres by Lerner *et al.* [39] find $\beta = 1/0.34 = 2.94$, while a later work of the same group, DeGiuli *et al.* [21], finds $\beta = 1/0.36 = 2.8$. Simulations on soft-core spheres by Kawaski *et al.* [40] find $\beta = 1/0.391 = 2.56$. None of these works discuss the exponent y. More recent work by Olsson [23], using a scaling analysis that includes corrections-to-scaling, finds $\beta = 3.8 \pm 0.1$ and $y = 1.16 \pm 0.01$. Olsson has argued that other works find a smaller value of β because they do not probe close enough to the critical point. Given the disagreement among these values of β for 3D simple shearing, our value of $\beta \approx 3.1$ for compression-driven jamming could be consistent with a common universality class. The situation remains to be clarified. See our Supplemental Material [26] for a comparison of β with the marginal-stability predictions.

Note, the values of y that we find from compression are in reasonable agreement with the values found from shearing. That $y > 1$ for compression in both 2D and 3D is surprising since it has generally been believed [2,4] that $y = 1$ for our harmonic contact interaction.

The above results were obtained by averaging together independent runs at constant values of the packing ϕ. In our Supplemental Material [26] we repeat our scaling analysis, but averaging our runs at constant values of the average particle contact number Z. We find no difference in any of the critical parameters between these two methods of averaging.

To summarize, we have carried out simulations of compression-driven jamming in a model of frictionless soft-core spheres in suspension, in two and three dimensions. Using the compression rate $\dot{\epsilon}$ as a scaling variable, in addition to the distance to jamming $\delta\phi$, we find that the pressure, and hence the bulk viscosity ζ, obey a critical scaling law (1) of the same form as found previously for shear-driven jamming. A diverging ζ demonstrates that compression is characterized by a finite timescale that diverges as $\phi \to \phi_J$ from below. Unlike the claims in [33] for the relaxation time τ, where $\ln N$ finite-size effects were seen for $\phi \leqslant 0.83$ in 2D systems of size $N \geqslant 4096$, and for $\phi \leqslant 0.57$ in 3D systems of size $N \geqslant 1024$, we observe no such finite-size effects in the bulk viscosity ζ for the entire range of ϕ and $\dot{\epsilon}$ we have used in our systems with $N = 16\,384$ and $32\,768$. Our results indicate that isotropic, compression-driven jamming in 2D and 3D has different critical exponents. For 2D our results suggest that stress-isotropic, compression-driven jamming is in the same universality class as stress-anisotropic, shear-driven jamming. For 3D the situation is less clear, but our results could also be consistent with a common universality class.

We thank P. Olsson, T. A. Marschall, M. A. Moore, and H. Ikeda for helpful discussions. This work was supported by National Science Foundation Grant No. DMR-1809318. Computations were carried out at the Center for Integrated Research Computing at the University of Rochester.

[1] A. J. Liu and S. R. Nagel, The jamming transition and the marginally jammed solid, Annu. Rev. Condens. Matter Phys. **1**, 347 (2010).

[2] C. S. O'Hern, L. E. Silbert, A. J. Liu, and S. R. Nagel, Jamming at zero temperature and zero applied stress: The epitome of disorder, Phys. Rev. E **68**, 011306 (2003).

[3] M. Wyart, L. E. Silbert, S. R. Nagel, and T. A. Witten, Effects of compression on the vibrational modes of marginally jammed solids, Phys. Rev. E **72**, 051306 (2005).

[4] P. Chaudhuri, L. Berthier, and S. Sastry, Jamming Transitions in Amorphous Packings of Frictionless Spheres Occur Over a Continuous Range of Volume Fractions, Phys. Rev. Lett. **104**, 165701 (2010).

[5] M. Pica Ciamarra, A. Coniglio, and A. de Candia, Disordered jammed packings of frictionless spheres, Soft Matter **6**, 2975 (2010).

[6] D. Vågberg, P. Olsson, and S. Teitel, Glassiness, rigidity, and jamming of frictionless soft core disks, Phys. Rev. E **83**, 031307 (2011).

[7] P. Olsson and S. Teitel, Critical Scaling of Shear Viscosity at the Jamming Transition, Phys. Rev. Lett. **99**, 178001 (2007).

[8] P. Olsson and S. Teitel, Critical scaling of shearing rheology at the jamming transition of soft-core frictionless disks, Phys. Rev. E **83**, 030302(R) (2011).

[9] D. Vågberg, P. Olsson, and S. Teitel, Critical scaling of Bagnold rheology at the jamming transition of frictionless two-dimensional disks, Phys. Rev. E **93**, 052902 (2016).

[10] P. Olsson and S. Teitel, Herschel-Bulkley Shearing Rheology Near the Athermal Jamming Transition, Phys. Rev. Lett. **109**, 108001 (2012).

[11] T. Hatano, Scaling properties of granular rheology near the jamming transition, J. Phys. Soc. Jpn. **77**, 123002 (2008).

[12] T. Hatano, Growing length and time scales in a suspension of athermal particles, Phys. Rev. E **79**, 050301(R) (2009).

[13] T. Hatano, Critical scaling of granular rheology, Prog. Theor. Phys. Suppl. **184**, 143 (2010).

[14] M. Otsuki and H. Hayakawa, Critical behaviors of sheared frictionless granular materials near the jamming transition, Phys. Rev. E **80**, 011308 (2009).

[15] C. Heussinger and J.-L. Barrat, Jamming Transition as Probed by Quasistatic Shear Flow, Phys. Rev. Lett. **102**, 218303 (2009).

[16] C. Heussinger, P. Chaudhuri, and J.-L. Barrat, Fluctuations and correlations during the shear flow of elastic particles near the jamming transition, Soft Matter **6**, 3050 (2010).

[17] P. M. Chaiken and T. C. Lubensky, *Principles of Condensed Matter Physics* (Cambridge University Press, Cambridge, 1995), see Sec. 5.4.

[18] M. Baity-Jesi, C. P. Goodrich, A. J. Liu, S. R. Nagel, and J. P. Sethna, Emergent SO(3) symmetry of the frictionless shear jamming transition, J. Stat. Phys. **167**, 735 (2017).

[19] Y. Jin and H. Yoshino, A jamming plane of sphere packings, arXiv:2003.10814.

[20] P. Urbani and F. Zamponi, Shear Yielding and Shear Jamming of Dense Hard Sphere Glasses, Phys. Rev. Lett. **118**, 038001 (2017).

[21] E. DeGiuli, G. Düring, E. Lerner, and M. Wyart, Unified theory of inertial granular flows and non-Brownian suspensions, Phys. Rev. E **91**, 062206 (2015).

[22] G. Düring, E. Lerner, and M. Wyart, Effect of particle collisions in dense suspension flows, Phys. Rev. E **94**, 022601 (2016).

[23] P. Olsson, Dimensionality and Viscosity Exponent in Shear-Driven Jamming, Phys. Rev. Lett. **122**, 108003 (2019).

[24] P. Olsson, Relaxation times and rheology in dense athermal suspensions, Phys. Rev. E **91**, 062209 (2015).

[25] H. Ikeda, Relaxation time below jamming, J. Chem. Phys. **153**, 126102 (2020).

[26] See Supplemental Material at http://link.aps.org/supplemental/10.1103/PhysRevE.103.L040901 for details of our compression protocol, tests for the absence of finite-size effects, the fluctuations between different independent compression runs, the predictions of the marginal-stability analysis, and results when we average samples at constant average contact number Z, rather than at constant packing ϕ.

[27] K. N. Nordstrom, E. Verneuil, P. E. Arratia, A. Basu, Z. Zhang, A. G. Yodh, J. P. Gollub, and D. J. Durian, Microfluidic Rheology of Soft Colloids Above and Below Jamming, Phys. Rev. Lett. **105**, 175701 (2010).

[28] F. Boyer, É. Guazzelli, and O. Pouliquen, Unifying Suspension and Granular Rheology, Phys. Rev. Lett. **107**, 188301 (2011).

[29] J. Paredes, M. A. J. Michels, and D. Bonn, Rheology Across the Zero-Temperature Jamming Transition, Phys. Rev. Lett. **111**, 015701 (2013).

[30] M. Dinkgreve, J. Paredes, M. A. J. Michels, and D. Bonn, Universal rescaling of flow curves for yield-stress fluids close to jamming, Phys. Rev. E **92**, 012305 (2015); see Appendix C for a further literature review.

[31] M. Dinkgreve, M. A. J. Michels, T. G. Mason, and D. Bonn, Crossover Between Athermal Jamming and the Thermal Glass Transition of Suspensions, Phys. Rev. Lett. **121**, 228001 (2018).

[32] A. Ikeda, T. Kawasaki, L. Berthier, K. Saitoh, and T. Hatano, Universal Relaxation Dynamics of Sphere Packings Below Jamming, Phys. Rev. Lett. **124**, 058001 (2020).

[33] Y. Nishikawa, A. Ikeda, and L. Berthier, Relaxation dynamics of non-Brownian spheres below jamming, J. Stat. Phys. **182**, 37 (2021).

[34] Compression at a finite rate has been considered in A. Donev, F. H. Stillinger, and S. Torquato, Do Binary Hard Disks Exhibit an Ideal Glass Transition? Phys. Rev. Lett. **96**, 225502 (2006); F. Stillinger and S. Torquato, Configurational entropy of binary hard-disk glasses: Nonexistence of an ideal glass transition, J. Chem. Phys. **127**, 124509 (2007). However they studied inertial hard spheres with elastic collisions and an initial velocity distribution sampled at a finite temperature, as might describe a thermal glass; they did did not investigate the critical behavior at jamming.

[35] D. J. Durian, Foam Mechanics at the Bubble Scale, Phys. Rev. Lett. **75**, 4780 (1995); Bubble-scale model of foam mechanics: Melting, nonlinear behavior, and avalanches, Phys. Rev. E **55**, 1739 (1997).

[36] S. Tewari, D. Schiemann, D. J. Durian, C. M. Knobler, S. A. Langer, and A. J. Liu, Statistics of shear-induced rearrangements in a two-dimensional model foam, Phys. Rev. E **60**, 4385 (1999).

[37] B. Andreotti, J.-L. Barrat, and C. Heussinger, Shear Flow of Non-Brownian Suspensions Close to Jamming, Phys. Rev. Lett. **109**, 105901 (2012).

[38] D. Vågberg, P. Olsson, and S. Teitel, Universality of Jamming Criticality in Overdamped Shear-Driven Frictionless Disks, Phys. Rev. Lett. **113**, 148002 (2014).

[39] E. Lerner, G. Düring, and M. Wyart, A unified framework for non-Brownian suspension flows and soft amorphous solids, Proc. Natl. Acad. Sci. (USA) **109**, 4798 (2012).

[40] T. Kawasaki, D. Coslovich, A. Ikeda, and L. Berthier, Diverging viscosity and soft granular rheology in non-Brownian suspensions, Phys. Rev. E **91**, 012203 (2015).

[41] D. Vågberg, P. Olsson, and S. Teitel, Dissipation and Rheology of Sheared Soft-Core Frictionless Disks Below Jamming, Phys. Rev. Lett. **112**, 208303 (2014).

[42] See: https://lammps.sandia.gov/.

[43] C. S. O'Hern, S. A. Langer, A. J. Liu, and S. R. Nagel, Random Packings of Frictionless Particles, Phys. Rev. Lett. **88**, 075507 (2002).

[44] D. Vågberg, D. Valdez-Balderas, M. A. Moore, P. Olsson, and S. Teitel, Finite-size scaling at the jamming transition: Corrections to scaling and the correlation-length critical exponent, Phys. Rev. E **83**, 030303(R) (2011).